P4.25 EVALUATION OF THE AMSU LAND SURFACE TEMPERATURE ALGORITHM FOR SKIN AND SHELTER-AIR TEMPERATURE RETRIEVALS

Cezar Kongoli [12], Paul Pellegrino[12], Fuzhong Weng[2], Charlie Dean[12] and Ralph Ferraro[2]

[1]QSS Group, Inc., Lanham, MD

[2]NOAAA/NESDIS, Camp Springs, MD

1. INTRODUCTION

Accurate satellite retrievals of skin and shelter-air temperature (i.e., at 2 m height) over land are important for climate studies, weather prediction models and meteorological applications. Skin temperature measurements on the ground are not routinely available, whereas in-situ measurements of shelter-air temperature are routinely made over the US and other parts of the globe. However, retrievals from satellites offer coverage in time and space that cannot be matched with ground measurements.

The Advanced Microwave Sounding Unit (AMSU) land surface temperature algorithm utilizes the microwave window frequency channels at 23.8, 31.4 and 50.3 GHz (Table 1, channels 1, 2, and 3, respectively). These lower frequency channels achieve maximum penetration through clouds, thus enabling retrievals of land surface parameters in nearly all weather conditions.

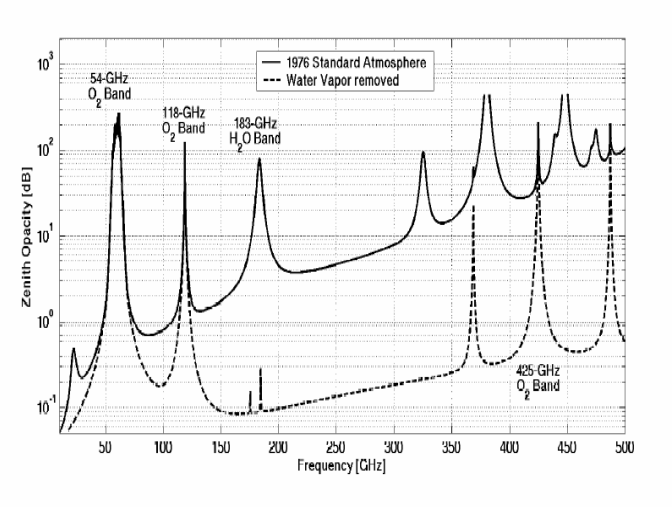

Figure 1. Zenith opacity in the 0-500 GHz frequency region (Chen, 2004).

Corresponding Author Address: Cezar Kongoli, NOAA/NESDIS, 5200 Auth Rd., 712, Camp Springs, MD 20746- 4304; E-mail: Cezar.Kongoli@noaa.gov

Channel number	Center frequency (GHz)	Number of pass bands	Band width (MHz)	Center frequency stability (MHz)
1	23.80	1	251	10
2	31.40	1	161	10
3	50.30	1	161	10
4	52.80	1	380	5
5	53.59±0.115	2	168	5
6	54.40	1	380	5
7	54.94	1	380	10
8	55.50	1	310	0.5
9	57.29 = fo	1	310	0.5
10	fo±0.217	2	76	0.5
11	fo±0.322 ±0.048	4	34	0.5
12	fo±0.322 ±0.022	4	15	0.5
13	fo±0.322 ±0.010	4	8	0.5
14	fo±0.322 ±0.004	4	3	0.5
15	89.00	1	2000	50
16	89.00	1	5000	50
17	150	1	4000	50
18	183±1	1	1000	50
19	183±3	2	2000	50
20	183±7	2	4000	50

Table 1. The AMSU frequency channel specifications

Figure 1 depicts the atmospheric opacity in the microwave frequency range between 0 and 500 GHz. For a standard atmosphere, atmospheric opacity is very low in the 20-50 GHz frequency range, and has a tendency to increase with increasing frequency even in the higher frequency window regions, e.g., 89-150 GHz for AMSU. In contrast, the land surface temperature retrievals from satellite IR measurements are affected by atmospheric clouds due to higher opacity and thus these retrievals deteriorate during cloudy conditions.

The AMSU land surface temperature algorithm has been developed from radiative transfer model calculations including land surface emissivities, with algorithm coefficients empirically adjusted for skin temperature retrievals.

The algorithm's expression for skin land surface temperature is of the following form:

$$T_s = a_0 + a_{11}*TB_1 + a_{12}*TB_1^2 + a_{21}*TB_2 + a_{22}TB_2^2 + a_{31}*TB_3 + a_{32}*TB_3^2 + a_z*\mu \quad \textbf{(1)}$$

Where:

T_s is the skin temperature, TB_1, TB_2 and TB_3 are the AMSU brightness temperatures at 23.8 (Table 1, channel 1), 31.4 (Table 1, channel 2), and 50.3 (Table 1, channel 3) GHz, μ is the cosine of the zenith angle. As above-mentioned, the algorithm's coefficients have been derived empirically from case studies using data from the Atmospheric Radiation Experiment (ARM), Southern Great Plains (SGP). It is important to note that of the three AMSU channels used in the algorithm, the 50.3 GHz window frequency channel provides the most correlation between the surface and overlying atmosphere.

The objective of this paper was to evaluate the AMSU land surface algorithm (eq. 1) for its ability to also retrieve shelter-air temperatures. The microwave retrievals of skin temperature from other sensors e.g., SSM/I (McFarland et al., 1990; Pulliainen et al., 1997; Basist et al., 1998) and AMSR (Njoku, 1999) have been reported in literature. Shelter-air temperatures, however, are also needed in a number of meteorological applications, e.g., estimation of near-surface sensible and latent heat fluxes.

The layout of this paper is as follows: Section 2 provides a detailed description of the data used in the study and the validation methodology. Section 3 provides a discussion of the validation results. And finally the "conclusions" section summarizes the paper and outlines future work.

2. DATA AND EVALUATION METHODOLOGY

The ground truth for algorithm evaluation were the standard hourly measurements of shelter-air temperature at 2 m height, obtained from the meteorological weather stations in the US, available at the NOAA's National Climatic Data Center (NCDC). The period of evaluation was the month of July and December 2002. The hourly observations of shelter-air temperature were collocated with daily AMSU satellite measurements from the NOAA-15, -16, and -17 satellites, descending and ascending passes. A detailed description of AMSU data and products generation is provided in Ferraro et al., 2002. This three-satellite suite provided approximately a 4-hour sampling interval per day. The collocation between ground-based stations and the AMSU centroid center was done for a ½ hour temporal and 60 km spatial maximum proximity.

Observations of shelter-air temperature are point measurements, whereas the AMSU measurements represent measurements integrated spatially over the instrument's field of view. Therefore, it was important to select a relatively flat homogenous area where point measurements are representative of a larger areal extent. The match-ups between the AMSU measurements and shelter-air temperature observations were thus subjected to a spatial filter. Match-ups were selected within the latitudes of 31 and 48 degrees north, and longitudes of 90 and 102.5 degrees west.

Another critical aspect of the algorithm evaluation was the identification of sources of confusion that impacted the AMSU measurements at the channel frequencies employed by the algorithm (Eq. 1). These sources include moderate to heavy precipitation, snow cover and wet soil (e.g., Grody 1991; Grody and Basist, 1996; Basist et al., 1998). In order to remove these sources of confusion, the following microwave screening procedure was applied to the match-ups, which utilized the AMSU-A channels at 23.8, 31.4 and 89 GHz frequencies (Table 1):

- Removal of snow signatures:
  $\mathbf{TB_{23}} <= 262$ K AND $\mathbf{TB_{23}}$-$\mathbf{TB_{89}} >= 4$ K **(2)**
- Removal of precipitation:
  $\mathbf{TB_{23}} > 262$ K AND $\mathbf{TB_{23}}$-$\mathbf{TB_{89}} >= 4$ K **(3)**
- Removal of wet areas:
  $\mathbf{TB_{23}} > 262$ K AND $\mathbf{TB_{23}}$-$\mathbf{TB_{89}} <= -8.0$ K **(4)**

Where **TB** in (2), (3) and (4) refers to the AMSU brightness temperature (in Kelvin) and the subscript refers to the channel frequency. The application of this screening algorithm to the match-up pairs removed 6687 match-ups, down to 27,477 pairs.

3. RESULTS AND DISCUSSION

Figures 2 and 3 depict scatter plots of the shelter-air temperature observations (referred to as Tobs) versus AMSU-estimated skin temperatures (referred to as Tsat). Un-filtered match-up pairs in Figure 2 refer to all the match-up pairs over the US Great Plains, whereas the filtered pairs in Figure 3 resulted from applying the conditions (2), (3) and (4).

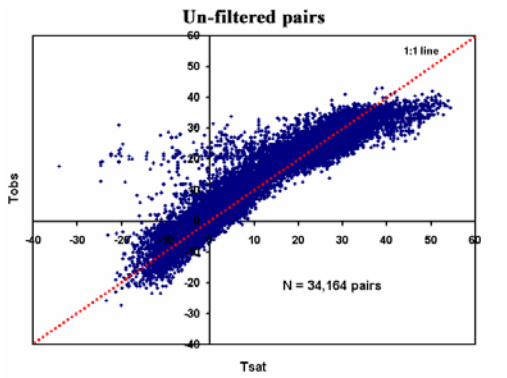

Figure 2. Scatter plot of the un-filtered match-up pairs between observed shelter-air temperatures (Tobs) and skin temperatures estimated by the AMSU algorithm (Tsat)

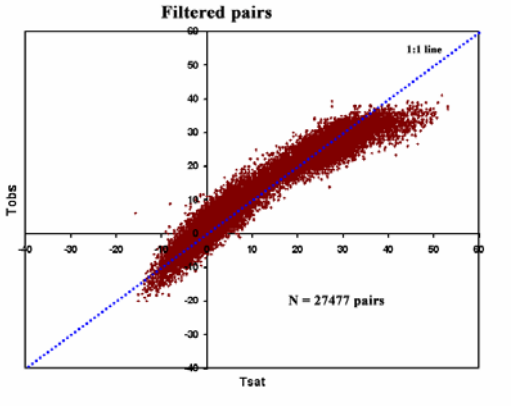

Figure 3. Scatter plot of all filtered match-up pairs between observed shelter-air temperatures (Tobs) and skin temperatures estimated by the AMSU algorithm (Tsat).

As shown, the outliers in Figure 2 were removed as a result of the screening procedure (Figure 3). These outliers were mainly due to snow cover and heavy precipitation. Figure 4 is a scatter plot of filtered pairs for the month of July (red-coded) and December (blue-coded). It is shown that the AMSU-estimated skin temperature and the observed shelter-air temperature follow a quadratic relationship, with the AMSU-estimated skin temperatures becoming higher than observed shelter-air as the temperatures increase. This response is realistic and is mainly due to seasonal differences in surface radiation patterns. For instance, during daytime in July, the skin temperature over land is generally warmer than shelter-air temperature due to surface warming caused by a positive flux of net radiation. During the winter, this difference between skin and shelter-air temperature is diminished due to reduced warming at the surface, and may become even negative, e.g., due to radiative cooling during cold, clear

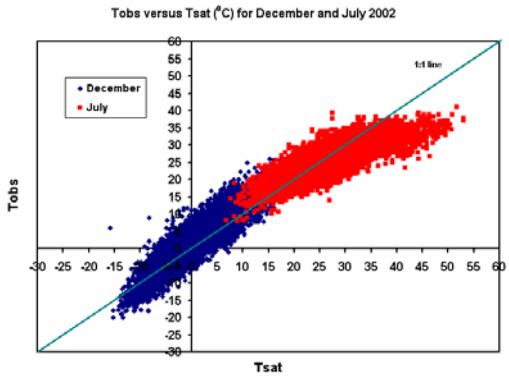

Figure 4. Scatter plot of filtered match-up pairs between observed shelter-air temperatures (Tobs) and skin temperatures estimated by the AMSU algorithm (Tsat) for July and December 2002

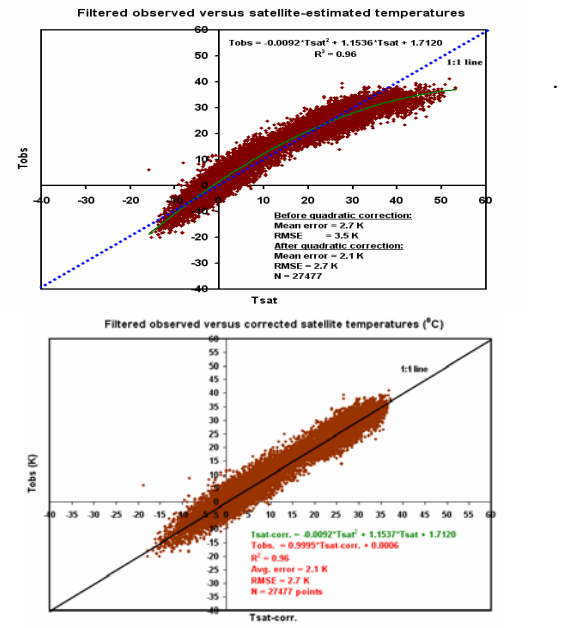

Figure 5. Scatter plot and summary statistics for filtered match-up pairs between observed shelter-air temperature and satellite-estimated skin temperature (top panel) and between shelter-air observed temperature and shelter-air satellite-estimated temperature converted from applying the quadratic relationship shown in the top panel.

nights. Figure 5 shows the statistics between the observed shelter-air and AMSU-estimated skin temperatures (top panel) and between the observed shelter-air and the shelter-air temperatures estimated from the AMSU. The bottom figure is the result of applying the quadratic correction to the AMSU-estimated skin temperature shown in the top panel. This quadratic conversion results in an average error of

2.1 K and Root Mean Square Error (RMSE) of 2.7 K, and a coefficient of determination of 0.96.

The one set of conversion coefficients derived from the entire filtered match-up pairs were applied to each satellite match-up dataset to estimate shelter-air temperature separately. Next, error statistics were computed for each satellite pass. It was found that satellite-specific biases still remain (Table 2), despite the removal of biases in the ensemble dataset. "Filtered-uncorrected" and "filtered-corrected" in Table 2 refer to match-up pairs between the AMSU-estimated skin and observed shelter-air temperatures and between the AMSU-estimated shelter-air and observed shelter-air temperatures, respectively. As Table 2 shows, satellite-specific biases between estimated and observed shelter-air temperatures remain in the "filtered corrected" match-ups, and in some cases, e.g. July NOAA-15 Ascending the bias deteriorated to -2 K. In order to remove satellite-specific biases, satellite-specific, quadratic conversion sets of coefficients were derived for each satellite pass (six sets). The results are summarized in Table 3. As shown, the application of satellite-specific conversion coefficients removed biases and further improved error statistics (Table 3). For instance, mean errors for "filtered-corrected" pairs were between 1.8 and 2.0 K, and RMSE between 2.3 and 2.5 K.

	FILTERED-UNCORRECTED			FILTERED-CORRECTED			
Satellite	*Bias*	*Mean error*	*RMSE*	*Bias*	*Mean error*	*RMSE*	*N*
July-N16-DES	0.7	1.9	2.4	1.0	1.8	2.2	2538
July-N16-ASC	2.3	3.5	4.7	-0.6	2.1	2.6	1231
July-N15-DES	1.3	2.6	3.3	0.6	1.9	2.3	2690
July-N15-ASC	-0.7	2.4	2.3	-2.0	2.5	2.3	2320
July-N17-DES	2.8	3.8	5.0	-0.2	1.9	2.4	2855
July-N17-ASC	1.2	2.3	2.9	0.6	1.7	2.1	2280
July-total	1.2	2.7	3.6	0.0	1.9	2.5	13915
DEC-N16-DES	-1.0	2.3	3.0	0.3	2.2	2.8	2276
DEC-N16-ASC	-3.1	3.4	4.2	-1.2	2.4	3.0	2360
DEC-N15-DES	-2.7	3.2	3.9	-1.1	2.4	3.1	2004
DEC-N15-ASC	-0.4	2.4	3.0	1.0	2.6	3.2	2106
DEC-N17-DES	-0.9	2.3	2.9	0.9	2.3	2.9	2603
DEC-N17-ASC	-1.2	2.4	3.0	0.2	2.2	2.7	2213
DEC-total	-1.6	2.7	3.4	0.0	2.3	2.9	13562
	Uncorrected-corrected						
Satellite	Mean error	RMSE					
July-N16-DES	0.1	0.2					
July-N16-ASC	1.4	2.1					
July-N15-DES	0.7	1.0					
July-N15-ASC	-0.1	0.0					
July-N17-DES	1.9	2.6					
July-N17-ASC	0.6	0.8					
July-total	0.8	1.1					
DEC-N16-DES	0.1	0.2					
DEC-N16-ASC	1.0	1.2					
DEC-N15-DES	0.8	0.8					
DEC-N15-ASC	-0.2	-0.2					
DEC-N17-DES	0.0	0.0					
DEC-N17-ASC	0.2	0.3					
DEC-total	0.4	0.5					
Coefficients	*a*Tsat2*	*b*Tsat*	*c*	*Corr (R2)*	*F-value*		
All-satellite	-0.0092	1.1536	17,120	0.96	0.00		

Table 2. Summary statistics for filtered match-up pairs of observed shelter-air and AMSU-estimated skin temperatures (referred to as "filtered-uncorrected"), and between observed and AMSU-estimated shelter-air temperatures (referred to as "filtered-corrected"). Only one set of regression coefficients was applied.

	FILTERED-UNCORRECTED			FILTERED-CORRECTED			
Satellite	*Bias*	*Mean error*	*RMSE*	*Bias*	*Mean error*	*RMSE*	*N*
N16-DES	-0.1	2.1	2.7	0.0	1.8	2.3	4814
N16-ASC	-1.3	3.5	4.4	0.0	2.1	2.6	3591
N15-DES	0.6	2.5	3.2	0.0	2.0	2.6	4796
N15-ASC	-1.6	2.8	3.5	0.0	2.0	2.6	4325
N17-DES	1.0	3.1	4.1	0.0	2.1	2.6	5458
N17-ASC	0.0	2.4	2.9	0.0	1.9	2.4	4493
Avg	-0.2	2.7	3.5	0.0	2.0	2.5	27477
Uncorrected - Corrected							
Satellite	*Mean error*	*RMSE*					
N16-DES	0.3	0.4					
N16-ASC	1.4	1.8					
N15-DES	0.5	0.6					
N15-ASC	0.8	0.9					
N17-DES	1.0	1.5					
N17-ASC	0.5	0.5					
Coefficient sets:							
Satelite	*a*Tsat2*	*b*Tsat*	*c*	*Corr. (R2)*	*F-value*		
N16-DES	-0.0103	1.1445	1.4304	0.96	0.00		
N16-ASC	-0.0111	1.1993	2.8413	0.96	0.00		
N15-DES	-0.0114	1.2050	1.0520	0.96	0.00		
N15-ASC	-0.0082	1.1448	3.0305	0.96	0.00		
N17-DES	-0.0111	1.2479	0.7590	0.96	0.00		
N17-ASC	-0.0083	1.1061	1.5622	0.96	0.00		

Table 3. Summary statistics for filtered match-up pairs of observed shelter-air and AMSU-estimated skin temperatures (referred to as "filtered-uncorrected"), and between observed and AMSU-estimated shelter-air temperatures (referred to as "filtered-corrected"). Six sets of regression coefficients (one per satellite pass) were applied.

4. CONCLUSIONS

Accurate satellite retrievals of skin and shelter-air temperature (i.e., at 2 m height) over land are important for climate studies, weather prediction models and meteorological applications. Retrievals from satellites offer coverage in time and space that cannot be matched with ground measurements.

The AMSU land surface algorithm was developed from radiative transfer model calculations using a multiple channel approach, with algorithm coefficients empirically adjusted for skin temperature retrievals. The objective of this paper was to evaluate the ability of the AMSU land surface algorithm to also retrieve shelter-air temperature retrievals. Shelter-air temperature observations were obtained from an extended network of in-situ meteorological stations over continental US and matched up with the AMSU measurements and estimated skin temperatures. Match-ups included microwave measurements from the three NOAA satellites, NOAA-15, -16, and -17, descending and ascending passes (approx. 4-hour sampling interval per day) in December and July, 2002. A microwave screening procedure was developed to remove effects of snow-cover, precipitation and surface wetness. Next, the screening algorithm was applied to the entire collocated match-up pairs. Statistical analysis of the

screened match-up pairs revealed a quadratic relationship between the observed shelter-air and the AMSU-estimated skin temperatures with a high coefficient of determination, standard error of 2.7 K and mean error of 2.1 K, a dramatic improvement of about 50% compared to errors associated with unscreened match-ups. The ensemble regression coefficients were applied to convert estimated skin temperatures into shelter-air temperatures. Comparisons between observed and AMSU-estimated shelter-air temperatures found remaining satellite-dependent biases despite improved retrieval errors, due to the diurnal temperature effects. To remove these remaining biases, regression coefficients were derived for each satellite from corresponding match-up pairs. As a result, the sheltered-air temperatures retrieved for each AMSU satellite pass were bias-free, with further reduced mean error of 2.0 K and RMSE of 2.5 K. Work is on-going to inter-compare the AMSU land surface temperature retrievals with those of the GOES satellite. Future work will also include tests of the AMSU land surface temperature algorithm with asymmetry correction in order to eliminate the angular dependent biases, and tests of limb-correction effects.

The views, opinions, and findings contained in this report are those of the author(s) and should not be construed as an official National Oceanic and Atmospheric Administration or U.S. Government position, policy, or decision.

5. REFERENCES

Basist, A.N., N.C. Grody, T Peterson, and C. Williams, 1998: Using SSM/I to monitor land surface temperature, wetness, and snow cover, *J. Applied Meteor., 37, 888-911.*

Chen, F.W., 2004: Global estimation of precipitation using microwave opaque bands (PhD thesis), *Massachusetts Institute of Technology, Massachusetts, USA*

Ferraro, R. R., F. Weng, N.C. Grody, I. Guch, C. Dean, C. Kongoli, H. Meng, P. Pellegrino, and L. Zhao, 2002: NOAA satellite-derived hydrological products prove their worth, *Eos Trans. AGU, 83*, 429-437.

Grody, N.C., 1991: Classification of snow cover and precipitation using the special sensor microwave imager*, J. Geophys. Res., 96(D4)*, 7423-7435.

Grody, N.C., and A.N. Basist, 1996: Global identification of snow cover using SSM/I Measurements, *IEEE Trans. Geosci. Remote Sens. 34(1)*, 237-249.

McFarland, M.J., R.L. Miller, and C.M.U. Neale, 1990: Land surface temperature derived from SSM/I microwave brightness temperature measurements, *IEEE Trans. Geosci. Remote Sens. 28*(5), *839-845.*

Njoku, E.G., 1999: AMSR land surface parameters: Algorithm theoretical basis document, Version 3.0, *Jet Propulsion Laboratory, Pasadena, CA.*

Pulliainen, J.T., J. Grandell, and M. T. Hallikainen, 1997: Retrieval of surface temperature from boreal forest zone from SSM/I data, *IEEE Trans. Geosci. Rem. Sens., 35, 1188-1200.*